Energy-dependent optimization of the prompt fission neutron spectrum with CGMF

Amy E. Lovell and Denise Neudecker

September 28, 2022

LA-UR-22-29989

1 Introduction

Throughout the course of FY21, significant effort was put into investigating models within the LANL-developed Hauser-Feshbach fission fragment decay code, CGMF [13], to understand and potentially solve the long-standing challenge of a too-soft prompt fission neutron spectrum, PFNS. Several inputs and models to CGMF were investigated, including the discrete nuclear levels, the optical model potential, level densities, and the fission fragment initial conditions [6]. Some of the global models within CGMF led to a slight hardening of the neutron spectrum—particularly the likely incomplete discrete levels in through which γ-rays decay—but none of the changes where large enough for the tail of the PFNS to reproduce experimental data. A significant hardening of the spectrum tail was observed when the fission fragment initial conditions were optimized based on their sensitivities to the PFNS data for thermal incident neutrons. In this way, the parameters for the CGMF mass and total kinetic energy distributions, along with the spin cutoff factor were adjusted to better reproduce the experimental PFNS measurements. This optimization hardened the tail of the PFNS slightly but led to unphysical mass distributions for the fission fragments before neutron emission.

It was clear from the above that we do not expect to be able to produce an evaluation-quality PFNS with CGMF in the near future. Challenges at thermal will persist–and possibly worsen–with increasing incident energy, where more models are needed to completely describe the fission. Basic-science research funding exceeding the amount available and scope of our NCSP funds would be needed to tackle this decade-long challenge impacting many fission-fragment event generator. And, in fact, Amy Lovell won LDRD ECR funding to do so over the next few years.

Therefore, we focused in FY22 on extending evaluation capabilities beyond thermal incident neutrons, to take into account the incident energy dependence of the PFNS and fission fragment initial condition distributions in CGMF. We chose to set up the evaluation methodology to perform PFNS evaluations with CGMF across incident-neutron energies, in order to have it readily available for future NCSP evaluations when the PFNS from CGMF has improved.

In this report, we outline the evaluation methodology, along with the results of the optimization, including full model calculations with CGMF using the evaluated parameters.

2 Evaluation

An evaluation of the ^{235}U PFNS was undertaken at incident-neutron energies, $E_{\rm inc}$, of thermal, 1.5, 6, and 14 MeV. PFNS at these $E_{\rm inc}$ were evaluated as (a) for thermal several experimental data set exist, (b) the importance of 1.5 and 14 MeV PFNS, and (c) to study whether we can fit second-chance fission structures seen in the PFNS at $E_{\rm inc}$ =6 MeV.

This evaluation uses CGMF model parameters, associated uncertainties, and CGMF-calculated PFNS values for all these $E_{\rm inc}$ as prior input. As mentioned previously, the aim was not to obtain evaluation-quality nuclear data, but rather to develop the methodology to undertake evaluations of PFNS at several $E_{\rm inc}$ based on the CGMF model at once.

Table 1: Experimental ^{235}U(n,f) PFNS used for this evaluation are identified by their first author, E_{out} and E_{inc} range.

E_{inc} First Author	E_{out} (MeV)	
thermal	Nefedov (anthracene) [14]	0.10854–1.91955
thermal	Nefedov (stilbene) [14]	1.013–7.84
thermal	Starostov [1]	4.115–12.06
thermal	Kornilov [4]	0.7–11.8
thermal	Vorobyev [15]	0.221–10.86
1.5 MeV	Knitter [3]	1.75–6.98
1.5 MeV	Lestone [5]	1.5–9.5
1.515 MeV	Chi-Nu [2]	0.211349–9.44061
6.006 MeV	Chi-Nu [2]	0.211349–9.44061
14.01 MeV	Chi-Nu [2]	0.211349–9.44061

2.1 Evaluation algorithm

For the study below, a new module, EvaluatKalmanPFNS.py, was implemented in the evaluation and experimental uncertainty quantification code ARIADNE [12]. This code relies on the Kalman filter technique that evaluates `CGMF` model parameters, $\boldsymbol{p}^{\boldsymbol{\psi}}$, and associated covariances, $\mathbf{Cov}^{\psi}$, by including initial model parameters, $\boldsymbol{p}^{\boldsymbol{\chi}}$, and covariances, $\mathbf{Cov}^{\chi}$, and experimental PFNS, $\boldsymbol{N}$, and their covariances $\mathbf{Cov}^{N}$, by:

$$\begin{aligned} \boldsymbol{p}^{\boldsymbol{\psi}} &= \boldsymbol{p}^{\boldsymbol{\chi}} + \mathbf{Cov}^{\psi}\boldsymbol{S}^{t}(\mathbf{Cov}^{N})^{-1}\left(\boldsymbol{N} - \boldsymbol{S}\boldsymbol{p}^{\boldsymbol{\chi}}\right), \\ \mathbf{Cov}^{\psi} &= \mathbf{Cov}^{\chi} - \mathbf{Cov}^{\chi}\boldsymbol{S}^{t}Q^{-1}\boldsymbol{S}\mathbf{Cov}^{\chi}, \end{aligned} \tag{1}$$

where

$$Q = \boldsymbol{S}\mathbf{Cov}^{\chi}\boldsymbol{S}^{t} + \mathbf{Cov}^{N}. \tag{2}$$

The evaluated model parameters, $\boldsymbol{p}^{\boldsymbol{\psi}}$, are forward-propagated to an evaluated PFNS, $\boldsymbol{\psi}$, by:

$$\boldsymbol{\psi} = \boldsymbol{\chi} + \boldsymbol{S}(\boldsymbol{p}^{\boldsymbol{\psi}} - \boldsymbol{p}^{\boldsymbol{\chi}}), \tag{3}$$

where $\boldsymbol{\chi}$ is the prior PFNS predicted by `CGMF` with the model parameters $\boldsymbol{p}^{\boldsymbol{\chi}}$.

Contrary to FY21 work, $\boldsymbol{N}$ and $\boldsymbol{\chi}$ are functions of E_{inc} and E_{out}. The shape of experimental PFNS, $\boldsymbol{N}$, of one data set at a selected E_{inc} must be rescaled with one multiplicative factor with respect to prior model data, $\boldsymbol{\chi}$, at the closest E_{inc}. This scaling factor was calculated by taking the ratio of numerical integrals of $\boldsymbol{\chi}$ and $\boldsymbol{N}$ for the same outgoing neutron energy range and the closest E_{inc} of model and experimental data. The variable $\boldsymbol{S}$ denotes sensitivities of model parameters to prior model PFNS $\boldsymbol{\chi}$ at specific E_{out} and E_{inc}. Hence, the code ARIADNE keeps track of the incident-neutron energy of experimental and model PFNS to correctly match them for the evaluation.

Also, iterative generalized least squares was implemented in ARIADNE to avoid Peelle's Pertinent Puzzle. This is described in more detail in Ref. [7].

2.2 Experimental input

We include the experimental data listed in Table 1. They are only described on a high level as they were accepted for the previous evaluation of the second author of the ^{235}U PFNS (see Fig. 3 in Ref. [10]) or are documented in Ref. [11]. The uncertainty estimate using the code ARIADNE [12] is described in detail in a laboratory report [8].

2.3 Model input

The input from the model in Eq. (1) comes in four forms:

- Initial model parameters, $\boldsymbol{p}^{\boldsymbol{\chi}}$, which are tabulated in Table 2,
- A covariances matrix associated with the initial model parameters, $\mathbf{Cov}^{\chi}$, that is diagonal with one-σ uncertainties defined in the third column of Table 2,

- prior PFNS values, $\boldsymbol{\chi}$, calculated with `CGMF` using $\boldsymbol{p^{\chi}}$ and shown in Section 2.4,
- sensitivities, $\boldsymbol{S}$, that link $\boldsymbol{p^{\chi}}$ and $\boldsymbol{\chi}$.

	First chance		Second chance		Third chance	
Parameter	Mean value	1-σ unc.	Mean value	1-σ unc.	Mean value	1-σ unc.
w_1^a	-6.8560	0.803	-31.1992	3.655	-30.1611	3.532
w_1^b	6.0824	0.766	30.0000	3.778	19.5576	2.463
μ_1^a	133.7900	1.951	133.60	1.951	132.68	1.951
μ_1^b	-0.2800	0.00748	-0.02	0.00748	-0.03	0.00748
σ_1^a	3.0288	0.984	3.7512	0.984	3.6964	0.984
σ_1^b	—	—	0.0823	0.0106	—	—
w_2^a	-6.8637	0.906	-30.5784	4.035	-29.5244	3.897
w_2^b	-6.1438	0.734	-29.8655	3.568	-19.3867	2.315
μ_2^a	140.9700	0.507	141.12	0.507	140.31	0.507
μ_2^b	-0.2700	0.00842	-0.04	0.00842	-0.05	0.00842
σ_2^a	4.6942	0.288	5.0365	0.288	5.1072	0.288
σ_2^b	0.1853	0.0106	0.1092	0.0106	0.0251	0.0106
σ_0^a	9.8854	0.142	10.0108	0.142	10.3022	0.142
σ_0^b	0.0322	0.000881	0.1089	0.00298	—	—
a	171.7400	4.0	170.09	4.0	170.6500	4.0
E_0	0.75	0.204	—	—	—	—
b	0.1718	0.178	—	—	—	—
d	-0.0975	0.210	-0.2371	0.210	-0.0557	0.0570
$A_m(TKE)$	131.7000	0.851	130.00	0.851	129.50	0.851
$A_{max}(TKE)$	166.0000	2.924	165.0000	2.924	160.0000	2.924
a_0	178.3800	0.752	178.11	0.752	178.5600	0.752
a_1	-0.3810	0.0522	-0.46732	0.0522	0.026447	0.0522
a_2	-0.14501	0.0224	-0.01245	0.0224	-0.10082	0.0224
a_3	0.0059204	0.00233	0.0038795	0.00233	0.0041158	0.00233
a_4	2.0923e-4	2.74e-5	6.5033e-5	2.74e-5	-6.1962e-5	2.74e-5
a_5	-1.6306e-5	5.86e-6	—	—	—	—
a_6	2.407e-7	6.44e-8	—	—	—	—
$A_m(sTKE)$	125.7500	7.657	126.0000	7.657	125.0000	7.657
$A_{max}(sTKE)$	163.0000	17.540	165.0000	17.540	155.0000	17.540
b_0	9.3499	1.483	7.5050	1.483	8.6246	1.483
b_1	-0.3200	0.0699	0.1753	0.0699	-0.096981	0.0699
b_2	0.0041924	0.000598	-0.027636	0.000598	-0.0062345	0.000598
b_3	1.9662e-4	1.96e-5	9.5005e-4	1.96e-5	1.96e-4	1.96e-5
b_4	-4.1142e-6	6.32e-7	-1.0120e-5	6.32e-7	—	—
α_0	1.4500	0.338	1.5800	0.0372	1.5000	0.0394
α_1	0.0700	0.151	0.0710	0.151	0.0710	0.151

Table 2: List of initial model parameter $\boldsymbol{p^{\chi}}$ and associated 1-σ uncertainties for first-chance, second-chance, and third-chance fission (^{236}U, ^{235}U, and ^{234}U compounds). Note that a bend in the TKE parametrization is only considered for first-chance fission and some parameters are zero (indicated by —) in the various fission chances.

Sensitivities and prior PFNS were calculated for ^{235}U PFNS induced by thermal neutrons using the same parameterization that we used in Ref. [9] for the evaluation of the ^{235}U(n,f) $\overline{\nu}$ without a bend in the average total kinetic energy as a function of incident-neutron energy. The same parameterization as for one of the $\overline{\nu}$ evaluations was chosen to understand if the same or different parameters change. Again, we take the three-σ uncertainties provided by the first author as one-σ uncertainties for the evaluation to test a large parameter space for possible better solutions of the PFNS.

One thing to note is that only 500k events were run to obtain these sensitivities. Hence, $\boldsymbol{S}$ and $\boldsymbol{\chi}$ below 0.005 MeV and above 15 MeV outgoing energy are not fully converged as can be seen in Fig. 1. As this evaluation was only undertaken to gain an understanding what parameters are changed to better agree to experimental data, it is not important to have fully converged PFNS in the wings.

2.4 Evaluated results

Evaluated PFNS, uncertainties, and model parameters are shown in Figs. 1, 2 and 3. The evaluated PFNS are shown for various numbers of GLS iterations that should address PPP (Peelle's Pertinent Puzzle), namely, none, 10, or 60 iterations. Different number of iterations were explored as the evaluated parameters changed distinctly if no versus 1-GLS iteration PPP correction was undertaken, and it was suspected that the missing PPP correction might adversely impact the evaluated PFNS. While there are noticeable differences in the evaluated PFNS with different number of iterations of GLS correcting for PPP, the differences are too small to explain why the evaluated PFNS differs distinctly from experimental data.

The PFNS evaluated using `CGMF` at thermal (Fig. 1) is reasonably smooth but distinctly too low below 1 MeV and above 5 MeV, and is too high at 2 MeV. The evaluated PFNS differs not only at thermal from experimental PFNS but for all other incident-neutron energies studied: the PFNS is in general too low below 1 MeV and above 8 MeV, while being too high around 2 MeV for all studied incident-neutron energies. At $E_{\rm inc}$ =1.5, 6, and 14 MeV, we also observe non-smooth behavior in the evaluated PFNS at all outgoing neutron energies. This could be either caused by that the `CGMF` evaluations need a denser grid of experimental data, or that the sensitivities of model parameters to prior PFNS have large uncertainties. These uncertainties would be larger at higher $E_{\rm inc}$, explaining the wiggles in evaluated data with increasing $E_{\rm inc}$, and especially at outgoing-neutron energies where the PFNS is small. To test this out, an evaluation with dense pseudo-experimental data was undertaken below. More specifically, we took as experimental input evaluated ^{235}U PFNS of an ENDF/B-VIII.1 release candidate [11].

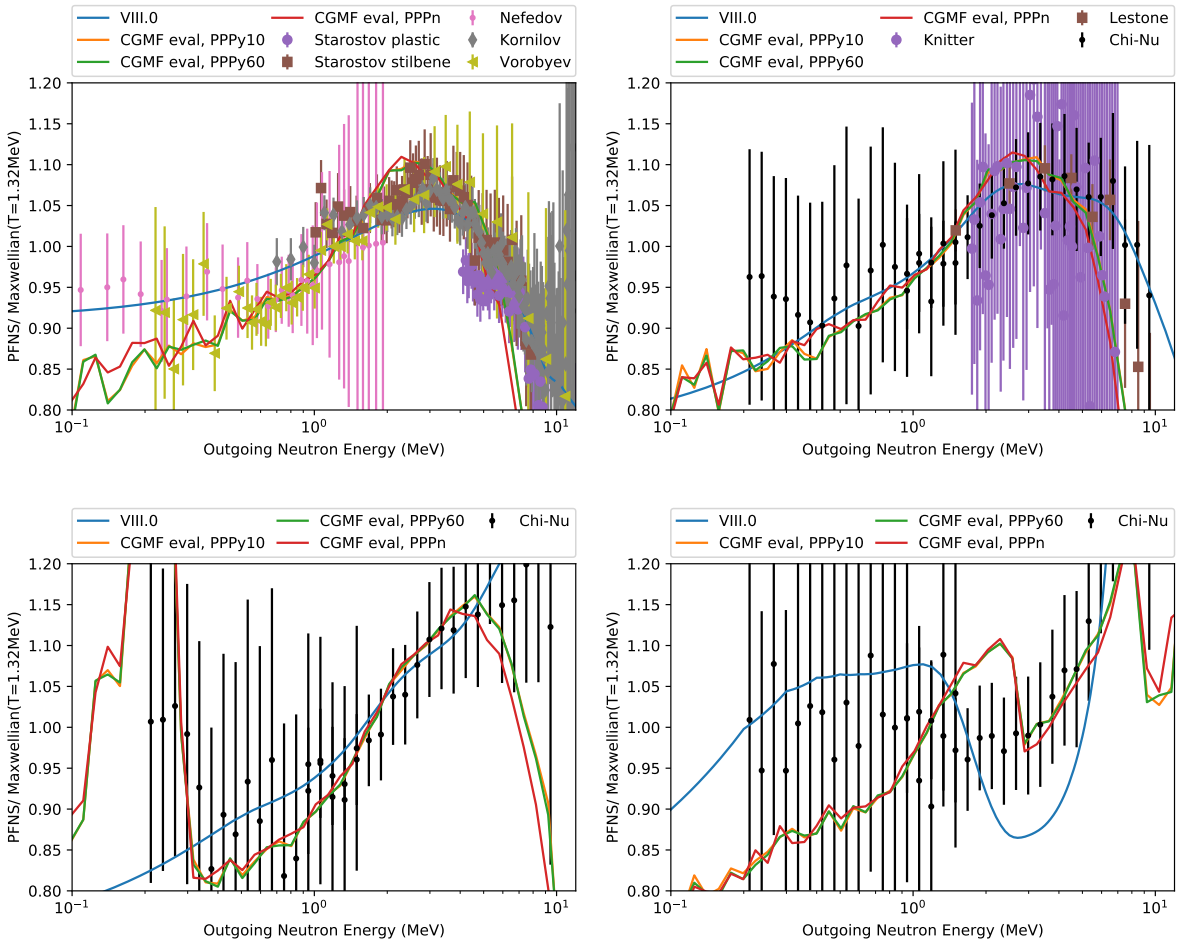

Figure 1: Evaluated ^{235}U PFNS at thermal, 1.5, 6, and 14 MeV incident neutron energies are compared to experimental data, and ENDF/B-VIII.0 for various outgoing neutron energies. The data were predicted with CGMF with different evaluated parameter sets.

The evaluated uncertainties shown in Fig. 2 are too low at thermal compared to experimental uncertainties entering the evaluation. They are more realistic for incident-neutron energies of 1.5 and 14 MeV,

but are too low for 6 MeV. This also illustrates that the prior parameter space does not fully capture the experimental data, and might also be too constraining.

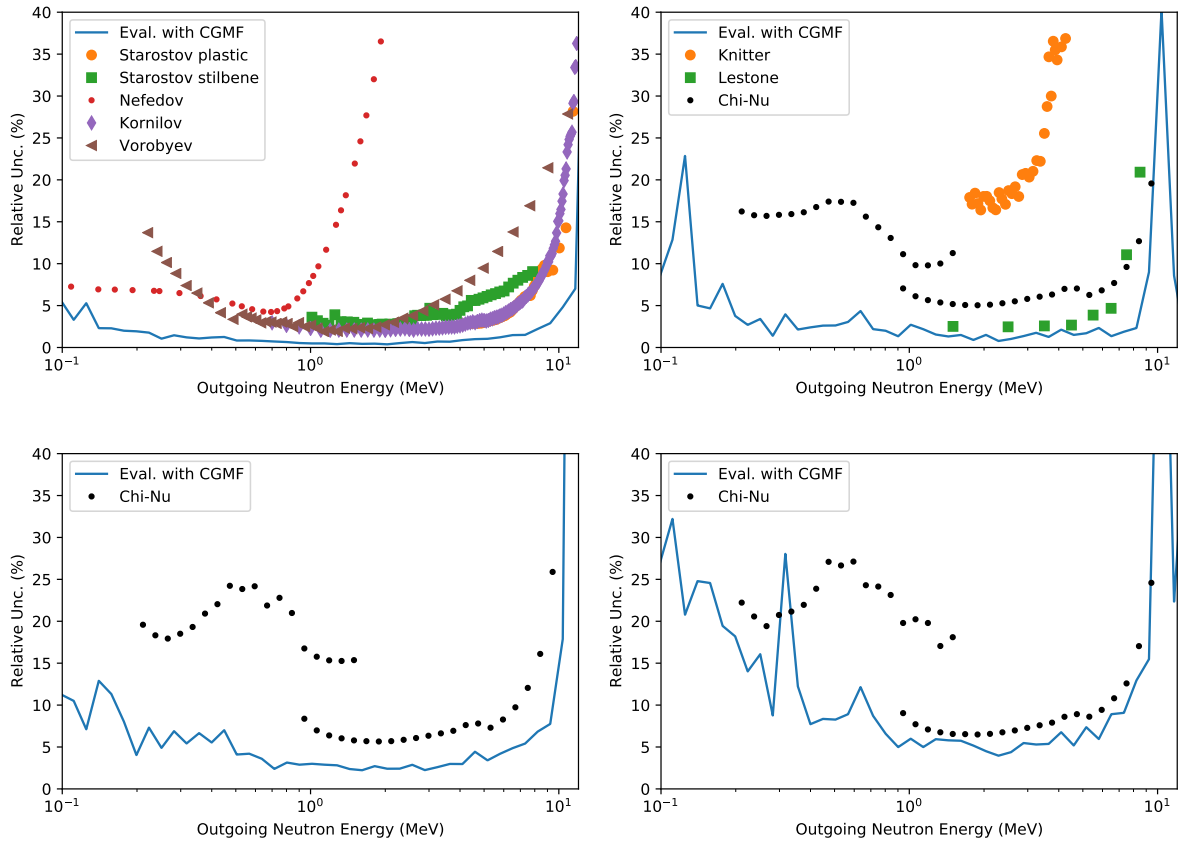

Figure 2: Evaluated ^{235}U PFNS relative uncertainties at thermal, 1.5, 6, and 14 MeV incident-neutron energies are compared to experimental uncertainties for various outgoing neutron energies. A PPP correction was undertaken with 60 GLS iterations.

The evaluated parameter changes shown in Fig. 3 are mostly within 25% of the prior value. The one exception is α_1 that changes distinctly, but little is known about this spin-cut off parameter.

In Fig. 4 `CGMF` parameters were fitted to an ENDF/B-VIII.1 release candidate of the ^{235}U PFNS [11] rather than experimental data. This evaluation tests whether a denser grid of pseudo-experimental data could remove non-smooth structures in the evaluated PFNS above thermal. While the evaluated PFNS get closer to ENDF/B-VIII.1 than previously, it cannot fit closely to them leading to erratic behavior for the evaluated PFNS including `CGMF` at E_{inc} =14 MeV. One can also still observe non-smooth structures in the evaluated PFNS. This points to that these wiggles in evaluated PFNS could be caused by too high uncertainties in the sensitivities, Amy Lovell tried to supply more precise sensitivities. However, `CGMF` evaluations timed out on a cluster due to the long time needed to calculate them. Hence, either `CGMF` calculations need to be sped up, or an emulator must be built.

In summary, we were able to evaluate PFNS with `CGMF` at multiple incident-neutron energies. Not surprisingly, the evaluated PFNS are distinctly too soft pointing to a well-known, but poorly understood, defect in the model. In addition to that it was shown that higher precision of sensitivities are needed to produce smooth evaluated PFNS. Both shortcomings need future development on `CGMF` going beyond NCSP funding.

2.5 Comparison of other prompt observables

We now run `CGMF` using the updated parameters to calculate the PFNS and other prompt fission observables. We show the comparison between the four optimizations: i) without the PPP correction (no PPP, typically black solid in all figures), with 10 PPP iterations (10 PPP, red dashed), with 60 PPP iterations (60 PPP, blue dotted), and for the fit to the ENDF/B-VIII.1 release candidate (ENDF/B-VIII.1, green dash dotted).

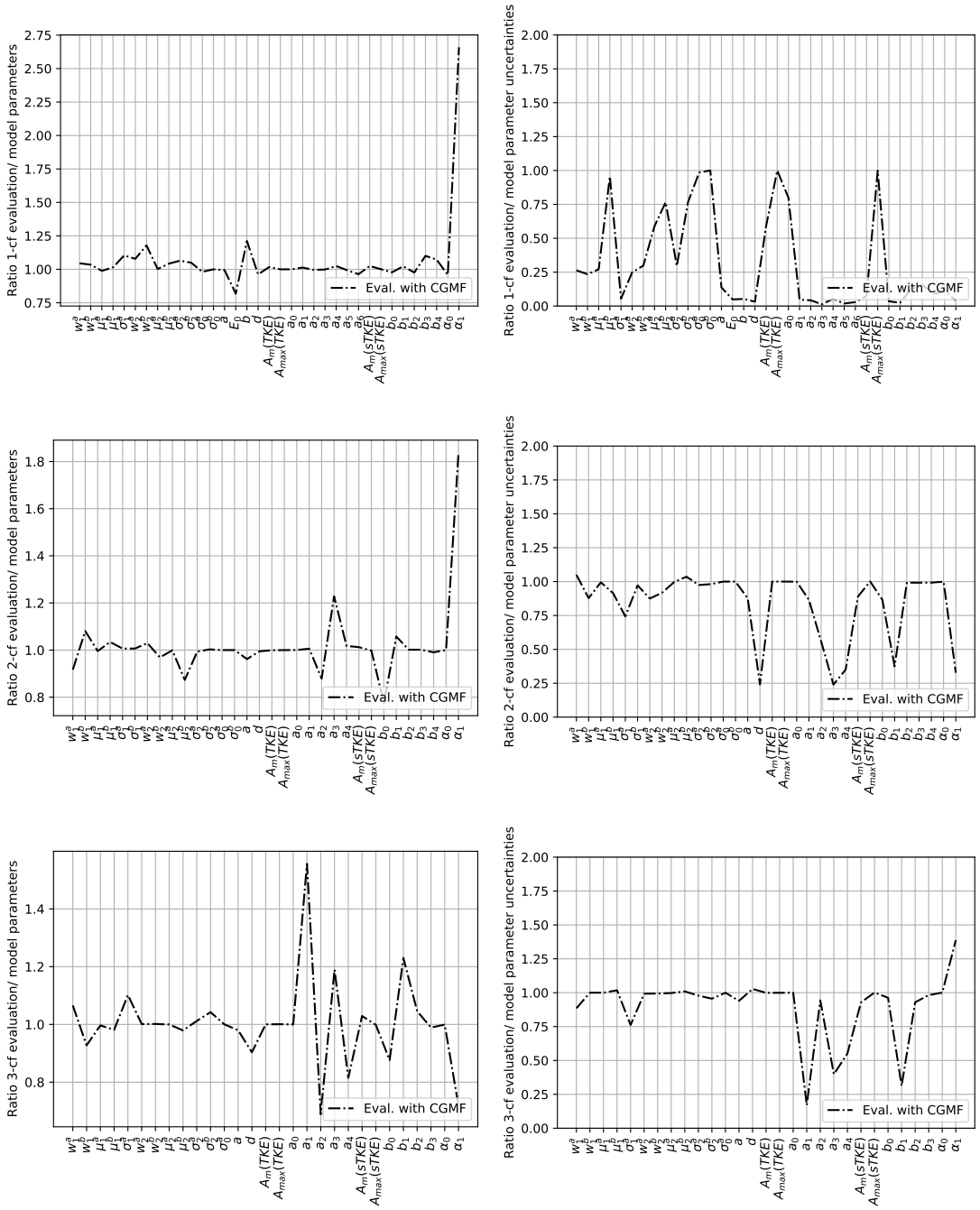

Figure 3: Change of evaluated parameters compared to prior parameters if they are fitted to experimental ^{235}U PFNS at thermal, 1.5, 6, and 14 MeV incident-neutron energies. Changes in 1st, 2nd and 3rd-chance fission parameters are shown. A PPP correction was undertaken with 60 GLS iterations.

In Fig. 5, we show a comparison among the optimizations for the pre-neutron emission mass distributions, $Y(A)$, at the incident neutron energies considered in the fit. The four `CGMF` results all show the expected trends as the incident energy increases–the symmetric mass region fills in–however, the fit to the ENDF/B-VIII.1 candidate release PFNS has a distinctly different shape, especially past first-chance fission, than the other three calculations.

In Fig. 6, we show the average prompt neutron and γ-ray multiplicities (top) and outgoing energies (bottom) for the four `CGMF` calculations compared to available experimental data. Note that, for each of the sub-plots, there are only four incident energy values (thermal, 1.5 MeV, 6.5 MeV, and 14.5 MeV) so the lines in between these points are meant to guide the eye and do not necessary accurately depict the energy-dependent trends (e.g. features at the openings of the multi-chance fission channels could be

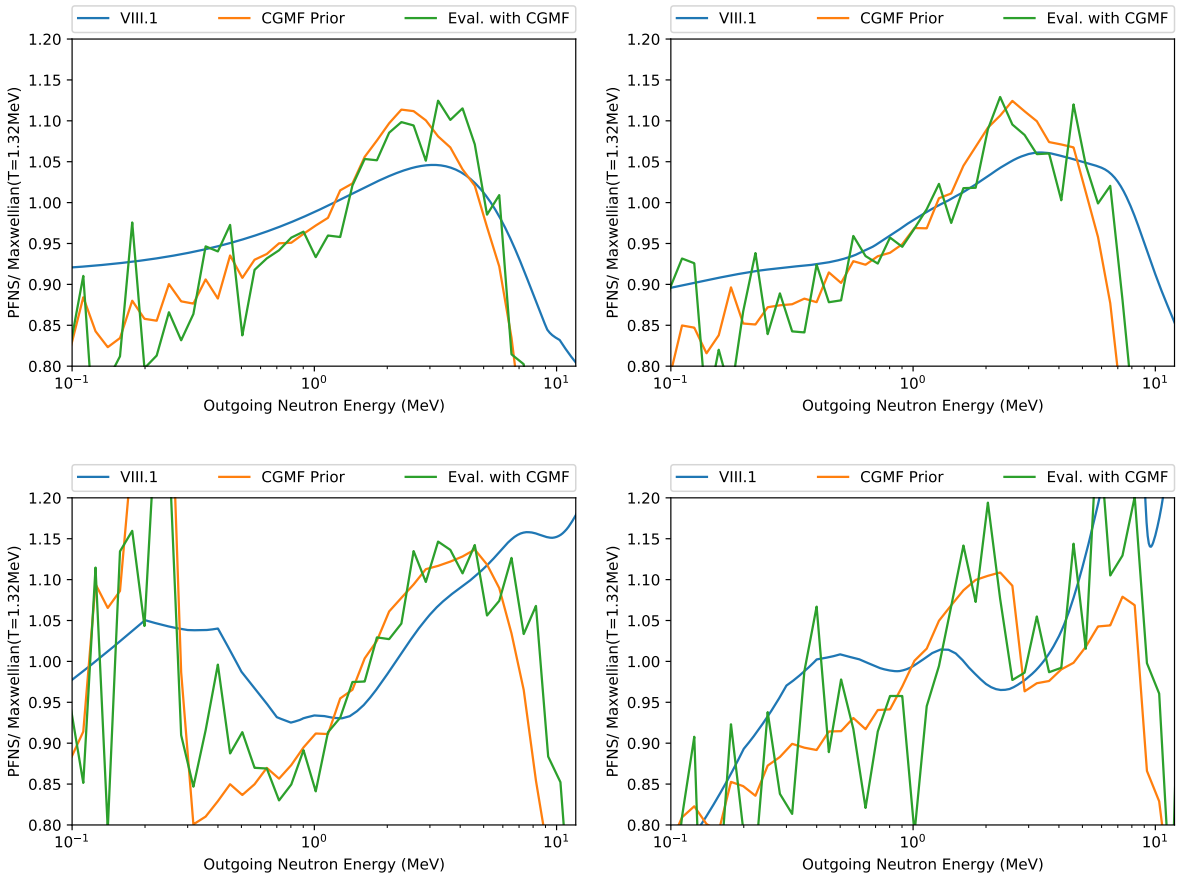

Figure 4: Evaluated ^{235}U PFNS at thermal, 1.5, 6, and 14 MeV incident-neutron energies are compared to prior PFNS and ENDF/B-VIII.1 for various outgoing neutron energies. PPP correction was not undertaken. `CGMF` parameters were fitted to ENDF/B-VIII.1 ^{235}U PFNS [11] rather than experimental data.

missing). Interestingly, for the neutron and γ-ray multiplicities, the fit to the ENDF/B-VIII.1 release candidate shows the largest discrepancy compared to the other three optimizations. The energy trends, on the other hand, are fairly similar; though it is important to note that the fit to the ENDF/B-VIII.1 candidate and the two fits with non-zero PPP corrections appear to reproduce the expected average outgoing neutron energy, which has typically been too low for Hauser-Feshbach models, even if the PFNS is still too soft.

Finally, in Fig. 7, we show the neutron and γ-ray multiplicity distributions, $P(\nu)$ and $P(N_\gamma)$, for thermal incident neutrons. The four optimizations produce essentially the same $P(N_\gamma)$ at thermal, although slight changes as a function of incident neutron energy can be more directly compared when fitting the distributions to a negative binomial and comparing the extracted parameters (not shown in this report). For each of the fits, besides the one without the PPP correction, the number of events with 3 neutrons emitted is larger than the number of events with 2 neutrons emitted, contrary to the trend seen in experimental data. The fit to the ENDF/B-VIII.1 release candidate shows the largest variation compared to the experimental data, and the shape of $P(\nu)$–although not shown here–becomes unphysical as the incident neutron energy increases.

3 Conclusion

In spring of FY22, Amy Lovell and Denise Neudecker had a discussion with Robert C. Little and Jennifer Alwin who lead the NCSP (Nuclear Criticality Safety Program) project funding nuclear data work at LANL on progress on meeting `CGMF`-related NCSP milestones. While it was shown that `CGMF` is able to evaluate the average prompt neutron multiplicity, $\overline{\nu}_p$, such that the resulting data closely mirror experimental data and are of sufficient quality that ^{235}U and ^{239}Pu $\overline{\nu}_p$ are ENDF/B-VIII.1 release

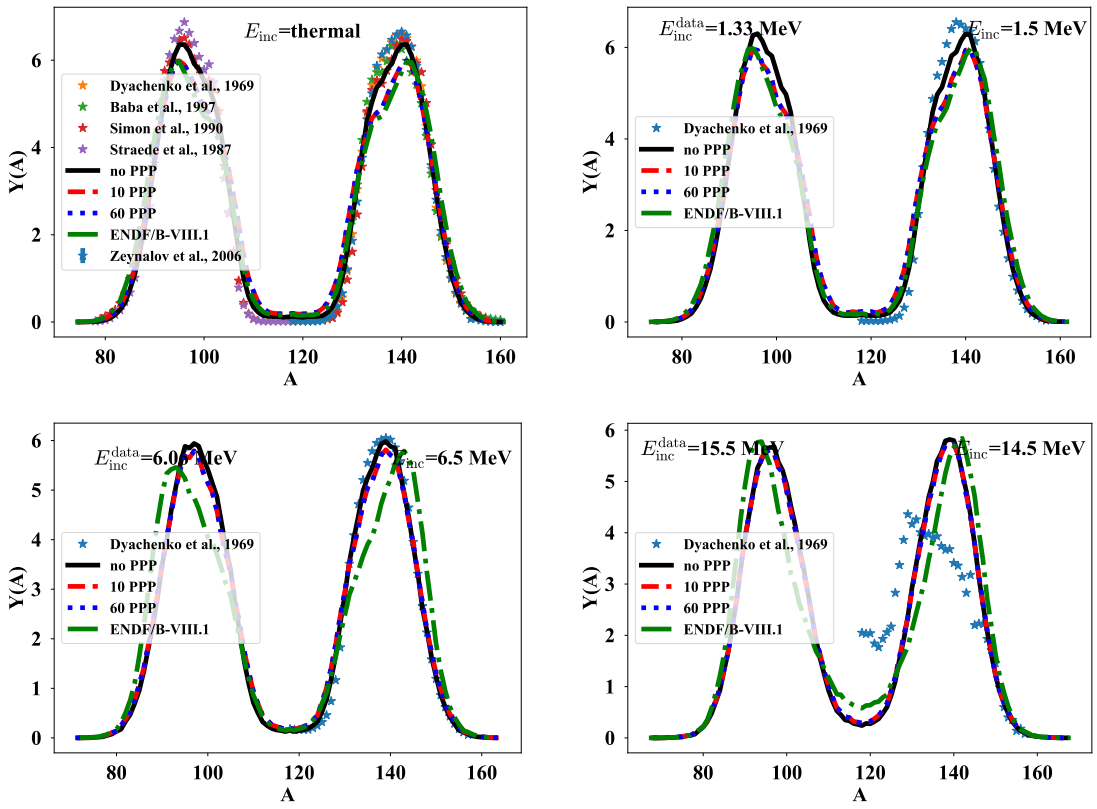

Figure 5: Comparison among the four PFNS optimization and available experimental data for the pre-neutron emission mass distribution, $Y(A)$, for incident neutron energies of thermal (upper left), 1.5 MeV (upper right), 6.5 MeV (lower left), and 14.5 MeV (lower right).

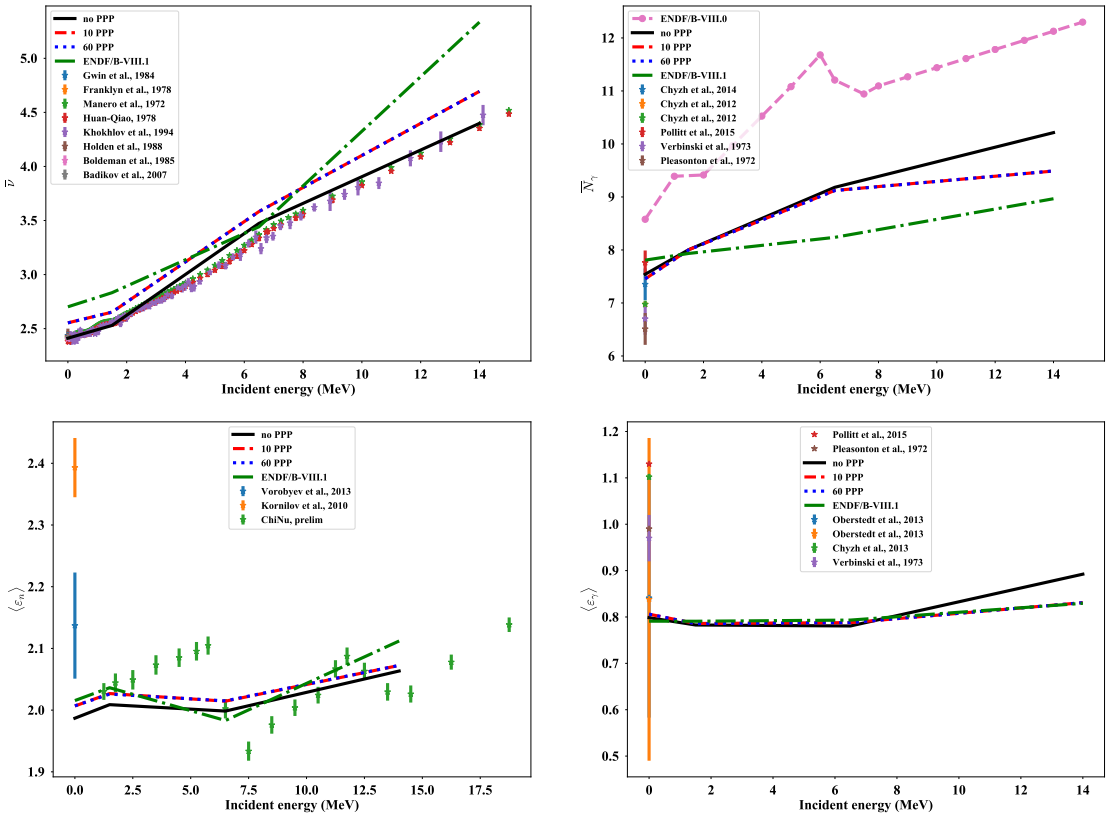

Figure 6: Average prompt (upper left) neutron and (upper right) γ-ray multiplicities for the four CGMF optimizations compared to experimental data. Average prompt outgoing (lower left) neutron and (lower right) γ-ray energies for the four CGMF optimizations compared to available experimental data.

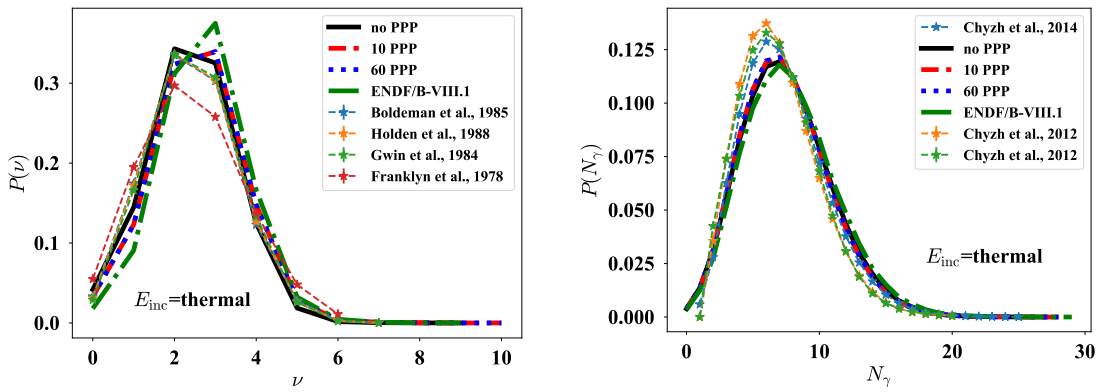

Figure 7: Prompt (left) neutron and (right) γ-ray multiplicity distributions with thermal incident neutrons for the four optimizations in CGMF compared to available experimental data.

candidates, the prompt fission neutron spectrum, PFNS, resulting from CGMF is too far from experimental data to be of evaluation quality.

However, there was a FY22 NCSP milestones for LANL that requires: "^{235}U, ^{239}Pu: Evaluate PFNS and multiplicity consistently, including angular information about prompt neutrons". We did evaluate ^{239}Pu $\overline{\nu}_p$ and ^{235}U $\overline{\nu}_p$ with CGMF and obtained through the consistent fission modeling of this code, evaluated PFNS and angular information in line with $\overline{\nu}_p$. This way we satisfied the milestone, which does not specify if the results should be of evaluation quality. This formulation was on purpose as CGMF is a research code and it was unclear if it would yield evaluated results of sufficient quality.

It is clear from the results above, that the evaluated PFNS obtained here are too soft. Ultimately, to produce an evaluation-quality PFNS, the underlying challenge of a too-soft PFNS will have to be solved. This solution will require a more dedicated effort on the modeling side of CGMF, which is outside of the current scope of our NSCP deliverables. Amy Lovell has an LDRD-ECR ongoing that will tackle this long-standing problem.

In the mean-time, it was discussed with Robert C. Little and Jennifer Alwin that we should generate for future NCSP evaluations the infrastructure to evaluated PFNS with CGMF as a function of incident neutron energy. This infrastructure was put in place and is documented in this report, thus satisfying the needs of the NCSP project. To showcase how this infrastructure worked, PFNS were evaluated with CGMF at incident-neutron energies of thermal, 1.5, 6 and 14 MeV. The evaluation code worked as expected, but, still, the PFNS was too soft. In addition, it was found out that the sensitivities of CGMF model parameters to predicted PFNS were too uncertain to evaluate a smooth evaluated PFNS. This is caused by the stochastic nature of the CGMF code that samples the PFNS. Subsequent efforts to increase the statistics were unsuccessful so far, and require more effort on speeding up CGMF as well as emulating the code.

References

[1] V.N. Nefedov B.I. Starostov and A.A. Boytsov. Precision measurements of ^{252}cf, ^{233}u+n_{th}, ^{235}u+n_{th} and ^{239}pu+n_{th} prompt fission neutron spectra (pfns) in the energy range 2–11 mev. Technical report, International Atomic Energy Agency Report INDC(CCP)-0458, 2014.

[2] K. J. Kelly, J. A. Gomez, M. Devlin, J. M. O'Donnell, D. Neudecker, et al. Measurement of the ^{235}U(n,f) Prompt Fission Neutron Spectrum from 10 keV to 10 MeV Induced by Neutrons of energy 1–20 MeV. *Phys. Rev. C*, 105:044615, 2022.

[3] H.-H. Knitter, M.M. Islam, and M. Coppola. Investigation of fast neutron interaction with ^{235}u. *Zeitschrift für Physik*, 257:108–123, 1972. EXFOR-No. 20394.008.

[4] N. Kornilov, F.-J. Hambsch, I. Fabry, S. Oberstedt, T. Belgya, Z. Kis, L. Szentmiklosi, and S. Simakov. The 235u(n, f) prompt fission neutron spectrum at 100 k input neutron energy. *Nuclear Science and Engineering*, 165(1):117–127, 2010.

[5] J.P. Lestone and E.F. Shores. Uranium and plutonium average prompt-fission neutron energy spectra (pfns) from the analysis of nts nuex data. *Nuclear Data Sheets*, 119:213–216, 2014.

[6] Amy E. Lovell and Denise Neudecker. Correcting the pfns for more consistent fission modeling. Technical report, Los Alamos National Laboratory Report LA-UR-21-30882, 2021.

[7] Amy Elizabeth Lovell, Denise Neudecker, and Patrick Talou. Release of evaluated ^{235}u(n,f) average prompt fission neutron multiplicities including the CGMF model. Technical Report LA-UR-22-23475, Los Alamos National Laboratory, 2022.

[8] D. Neudecker. Experimental data and covariances for evaluating the neutron-induced ^{235}u prompt fission neutron spectrum. Technical report, Los Alamos National Laboratory Report LA-UR-17-28970, 2017.

[9] D. Neudecker, A.E. Lovell, and P. Talou. Producing endf/b-quality evaluations of ^{239}pu(n,f) and ^{235}u(n,f) average prompt neutron multiplicities using the cgmf model. Technical report, Los Alamos Nat. Lab. LA-UR-21-29906, 2021.

[10] D. Neudecker, P. Talou, T. Kawano, A.C. Kahler, M.C. White, T.N. Taddeucci, R.C. Haight, B. Kiedrowski, J.M. O'Donnell, J.A. Gomez, K.J. Kelly, M. Devlin, and M.E. Rising. Evaluations of energy spectra of neutrons emitted promptly in neutron-induced fission of 235u and 239pu. *Nuclear Data Sheets*, 148:293–311, 2018. Special Issue on Nuclear Reaction Data.

[11] Denise Neudecker and Keegan John Kelly. Including chi-nu ^{235}u pfns experimental data into an endf/b-viii. 1 release candidate evaluation. Technical Report LA-UR-22-22220, Los Alamos National Laboratory, 2022.

[12] Neudecker, Denise. Ariadne - a program estimating covariances in detail for neutron experiments. *EPJ Nuclear Sci. Technol.*, 4:34, 2018.

[13] P. Talou, I. Stetcu, P. Jaffke, M.E. Rising, A.E. Lovell, and T. Kawano. Fission fragment decay simulations with the CGMF code. *Comput. Phys. Commun.*, 269:108087, 2021.

[14] B.I. Starostov V.N. Nefedov and A.A. Boytsov. Precision measurements of ^{252}cf, ^{233}u, ^{235}u and ^{239}pu prompt fission neutron spectra (pfns) in the energy range 0.04–5 mev. Technical report, International Atomic Energy Agency Report INDC(CCP)-0457, 2014.

[15] A.S. Vorobyev and O.A. Shcherbakov. Integral prompt neutron spectrum for fission of ^{235}u by thermal neutrons. Technical report, International Atomic Energy Agency Report Report INDC(CCP)-0455, 21–41, 2014.